buildings

MDPI

*Article*

# Research on Fatigue Performance of Shape-Memory Alloy Bars under Low Cyclic Loading

**Lei Li [1,*], Xianxian Zhao [2] and Junwei Cheng [2]**

[1] School of Civil Engineering Architecture, Zhengzhou University of Aeronautics, Zhengzhou 450046, China
[2] School of Materials, Zhengzhou University of Aeronautics, Zhengzhou 450046, China
* Correspondence: lileixiaozhou@163.com

**Abstract:** In recent years, shape memory alloys (SMAs) have been applied in the vibration control of engineering structures due to their special properties such as super elasticity and high damping, and the study of the performance of SMA wires has been relatively comprehensive, while research on the fatigue performance of SMA bars via cyclic tensile tests has been pretty rare, and low-cycle fatigue test has not been reported. However, the damage to building structures caused by earthquakes is of high-strain, low-cycle fatigue; therefore, in order for SMA bars to be used in seismic design, low-cycle fatigue tests were conducted on SMA bars with a diameter of 14 mm in this paper. Firstly, specimens were heat treated at a constant temperature of 350 °C for 30 min; other specimens were heat treated at a constant temperature of 400 °C for 15 min, while the rests were heat treated under a constant temperature of 400 °C for 30 min. Secondly, the energy dissipation capacity and residual strain of the SMA bar specimens were determined using the low-cycle fatigue test, in which the strain amplitudes were 2.5%, 3.5% and 3.75%. Additionally, the stress–strain relationship for SMA bars under cyclic loading was given. Finally, low-cycle fatigue properties of SMA bars were numerically simulated in the comparison analysis with the experimental results to verify their feasibility. Thus, it is proved that SMA bars can be recommend for seismic design building structures.

**Keywords:** shape-memory alloy; low-cycle fatigue; superelastic effect; re-centering effect



**Citation:** Li, L.; Zhao, X.; Cheng, J. Research on Fatigue Performance of Shape-Memory Alloy Bars under Low Cyclic Loading. *Buildings* **2023**, *13*, 1553. https://doi.org/10.3390/buildings13061553

Academic Editors: Rajai Zuheir Al-Rousan and Francisco López-Almansa

Received: 26 April 2023
Revised: 15 May 2023
Accepted: 12 June 2023
Published: 18 June 2023



## 1. Introduction

In recent years, earthquakes have occurred frequently, such as the Wenchuan earthquake in 2008, the Great Intelligence Earthquake in 2010, the Honshu Earthquake in 2011, and the Great Turkey Earthquake in 2023; they caused significant casualties and economic losses, and tens of thousands of buildings were damaged and collapsed. In the Turkey earthquake, buildings with strict seismic designs survived two consecutive 7.8 magnitude earthquakes, thus proving that the damage to buildings can be prevented and reduced. Under the action of high-strain and low-circumference earthquakes, fatigue damage occurs in a structure, and an earthquake causes high residual deformation or direct damage to traditional ductile members, making the structure difficult to recover after the earthquake, and even causing collapse damage to occur. Therefore, it is imperative to explore ductile and high-strength building materials and design functional members with recoverable performances. The early research on SMAs mainly focused on small-diameter wire: Graesser [1] studied the hysteresis model and cyclic tests of shape-memory alloys and modified the hysteresis model of SMAs. Piedboeuf [2] proposed a third harmonic Fourier sinusoidal series model to simulate the dynamic behavior of shape-memory alloys. Dolce [3] conducted cyclic tensile tests on SMA filaments to observe the changes in properties such as cut-line stiffness, energy loss, equivalent damping and residual strain during the tests. Gong [4,5] conducted an experimental study on the superelastic behavior of SMA wires under cyclic loading conditions with different temperatures and strain rates and suggested that pre-training can make the superelastic properties of SMA wires become stable. Sadiq [6]

investigated the effect of heat treatment parameters on the mechanical behavior of NiTi shape-memory alloy wires. Tamai [7] proposed a shape-memory alloy wire-based seismic member and studied the restoring force characteristics of the SMA wire. Zuo [8] investigated the effects of ambient temperature, strain amplitude, number of cycles and loading rate on the mechanical properties of SMA wire in a superelastic state. Qian [9] studied the mechanical properties of SMA wires, showing that the damping energy dissipation characteristics and self-resetting characteristics of SMA wires with diameters of 0.5 mm are better than SMA wires with diameters of 1.2 mm and 2.0 mm. Li [10] discussed the effects of strain amplitude and number of cyclic loadings on the maximum phase change strain of SMA wire. Yan [11] investigated the superelastic properties of SMA wires via cyclic tensile tests and compared the experimental results with Grasser's theoretical model.

However, due to the restoring force provided by SMA wire being limited and the application of bar-shaped members such as steel bars being more extensive in engineering practice, scholars at home and abroad have investigated the effects of different heat treatment conditions, strain amplitudes and loading rates on the mechanical properties of large-diameter SMA bars through torsional and cyclic tensile tests in recent years: Chen [12] studied the stress–strain behavior of shape-memory alloy bars at cyclic loading rates of 0.001–750 $s^{-1}$ and investigated the effect of loading rates on the mechanical properties of shape-memory alloys. Dolce [13] performed torsion tests on SMA bars. Desroches [14] conducted tests on SMA bars under quasi-static and dynamic loading, and the effect of bar size and loading history on its strength and equivalent viscous damping was investigated. Wang [15] discussed issues related to the heat treatment, mechanical property evaluation and joint design of SMA bars with a diameter of 14 mm. Zheng [16] obtained the relationship between the hyperelastic properties of SMA bars and the loading rate via cyclic tensile tests. Ren [17] found that the superelasticity of SMA bars decreases in cyclic loading and unloading, but the output force of 14 mm diameter bars is large. Dong [18] conducted experimental research on the heat treatment and material properties of SMA bars with a diameter of 14 mm and used it to develop a 25 mm diameter SMA self-resetting device. Kang [19] investigated the mechanical properties of shape-memory alloy bars with a diameter of 14 mm for different heat treatment processes. Wang [20] conducted superelasticity tests on SMA bars of different diameters with different loading regimes and proposed that the shape-memory alloy material can be made fully superelastic through "exercise". Zhuang [21] conducted mechanical tests on SMA bars of two chemical compositions and also simulated the mechanical properties with finite element software.

At present, most scholars have studied the fatigue properties of SMA via cyclic tensile tests, but the low-cycle fatigue properties of Ni-Ti shape-memory alloys are rarely studied. Therefore, in this paper, low-cycle fatigue tests are conducted on large-diameter SMA bars to study the effects of different heat treatment conditions and strain amplitudes on the energy dissipation capacity and recovery performance of SMA bars, which lay the foundation for the establishment of the fatigue damage model of shape-memory alloys.

## 2. Materials and Methods

### *2.1. Specimen Design and Experimental Materials*

The test was conducted using SMA bars with a diameter of 20 mm provided by Baoji Hai peng Metal Materials Co. The component content of the material is shown in Table 1. The critical phase transition temperature of the specimen was Af = 10 °C ± 5 °C, and the experimental temperature was 20 °C ± 3 °C, so the specimen was in an austenite state.

**Table 1.** Component content of SMA materials.

| Ti | Ni | Co | Cu | Cr | Fe | Nb | C | H | O | N |
|---|---|---|---|---|---|---|---|---|---|---|
| Remaining | 55.90 | 0.005 | 0.005 | 0.005 | 0.012 | 0.005 | 0.032 | 0.001 | 0.039 | 0.001 |

The SMA bars were designed and processed into the specimen shown in Figure 1 in accordance with GBT3075-2008 "Metallic Materials-Fatigue testing-Axial force-controlled method", and the specimens were heat treated at 350 °C (30 min), 400 °C (15 min) and 400 °C (30 min).


(**a**) (**b**)

**Figure 1.** Specimen for low circumference fatigue test. (**a**) Specimen size. (**b**) Specimen.

### *2.2. Experimental Equipment*

The test equipment was a model 370.25 MTS Landmark electro-hydraulic servo mechanics test system with a maximum rated load of 250 KN. The equipment is shown in Figure 2.

**Figure 2.** Test equipment.

### *2.3. Low-Cycle Fatigue Test Scheme*

The low-cycle fatigue test was carried out in accordance with GB/T 15248-2008 "The test method for axial loading constant-amplitude low-cycle fatigue of metallic materials". In order to study the effect of different strain amplitudes and heat treatment conditions on the fatigue performance of shape-memory alloys, the experimental parameters are listed in Table 2, and the test scheme was formulated as follows:

**Table 2.** Low-period fatigue experimental parameters.

| Specimen Number | Diameter (mm) | Heat Treatment Temperature (°C) | Heat Treatment Time (min) | Strain Amplitude (%) | Load Rate (Hz) |
|---|---|---|---|---|---|
| 1 | 14 | 350 | 30 | ±2.5 | 0.01 |
| 2 | 14 | 350 | 30 | ±3.5 | 0.01 |
| 3 | 14 | 350 | 30 | ±3.75 | 0.01 |
| 4 | 14 | 400 | 15 | ±2.5 | 0.01 |
| 5 | 14 | 400 | 30 | ±2.5 | 0.01 |

I: Three shape-memory alloy specimens (specimen 1–3) were taken and cyclically loaded at strain amplitudes of ±2.5%, ±3.5% and ±3.75% 30 times after being held at 350 °C for 30 min to analyze the low-cycle fatigue performance of the shape-memory alloy at different strain amplitudes.

II: The bars (specimen 4–5) held at 400 °C for 15 min and 400 °C for 30 min were cyclically loaded for 30 cycles with the strain amplitude of ±2.5%, and the test results were

compared with the test on bars held at 350 °C for 30 min to analyze the effect of different heat treatment conditions on the fatigue performance of the shape-memory alloy.

To reduce the measurement error caused by the loading rate, the loading frequency of the test was 0.01 Hz, and the waveform was a sine wave (as shown in Figure 3). According to the comparison of the specimen before and after loading (as shown in Figure 4), there was no obvious buckling of the specimen.

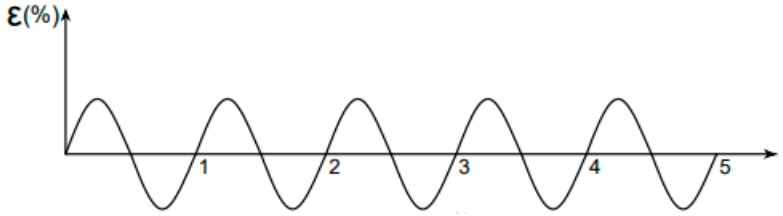


**Figure 3.** Loading waveform.

(**a**) (**b**)

**Figure 4.** Specimen for low-circumference fatigue test. (**a**) Before loop loading. (**b**) After 30 cycles.

## 3. Static Tensile Test

In this study, the peak tensile stress and the stress–strain relationship of the specimens were required for the low-circumference fatigue test study of the SMA bars. Therefore, a static tensile test was required. The test equipment was a MTS Landmark® electro-hydraulic servo test system, and the test was conducted in accordance with the requirements of GB/T228.1—2010 "Metallic materials-Tensile testing Part 1: Method of test at room temperature".

The static tensile test results of the SMA bar are shown in Table 3, and the stress–strain curves are shown in Figure 3. From Table 3 and Figure 5, it can be seen that the peak tensile stress of the SMA bar is 682.68 MPa and the elongation is 14.52%, which is within the 12% error with the quality inspection report data provided by the manufacturer. It can be seen that the SMA bar has stable performance, so the test data have good reliability and can be used as the basis for determining the bar's fatigue test parameters.

**Table 3.** Monotonic tensile test data of SMA bar.

| Items | Value |
|---|---|
| Yield strength ($f_y$) | 432.48 MPa |
| Yield strain ($\varepsilon_y$) | 3.75% |
| Elastic modulus ($E_s$) | 29,454 MPa |
| Strain of the intensive start phase ($\varepsilon_{sh}$) | 4.24% |
| Elastic modulus of the intensive start phase ($E_{sh}$) | 3292 MPa |
| Peak stress ($f_u$) | 682.68 MPa |
| Strain corresponding to the peak stress ($\varepsilon_u$) | 14.52% |

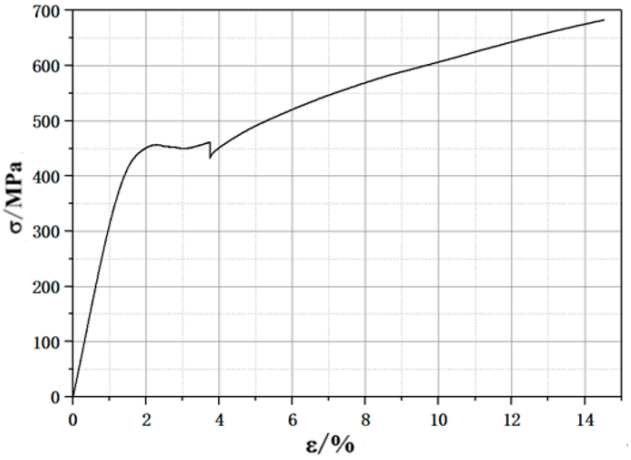


**Figure 5.** Monotonic tensile stress–strain curve of SMA bar.

## 4. Analysis of Low-Cycle Fatigue Test Results

### *4.1. Influence of Strain Amplitude on Superelasticity and Energy Consumption of SMA Bar*

Three shape-memory alloy bars (specimens 1–3) with the diameter of 14 mm and heat treatment parameters of being held at 350 °C for 30 min were selected for a low-cycle fatigue test with strain amplitudes of 2.5%, 3.5% and 3.75%, The stress–strain curves of the three specimens after 10 cycles at different strain amplitudes are shown in Figure 6. From Figure 6a–c, it can be seen that with the increase in strain amplitude, the area of hysteresis curve becomes larger, and the shape becomes full, which means that the energy dissipation capacity of the specimen is enhanced.

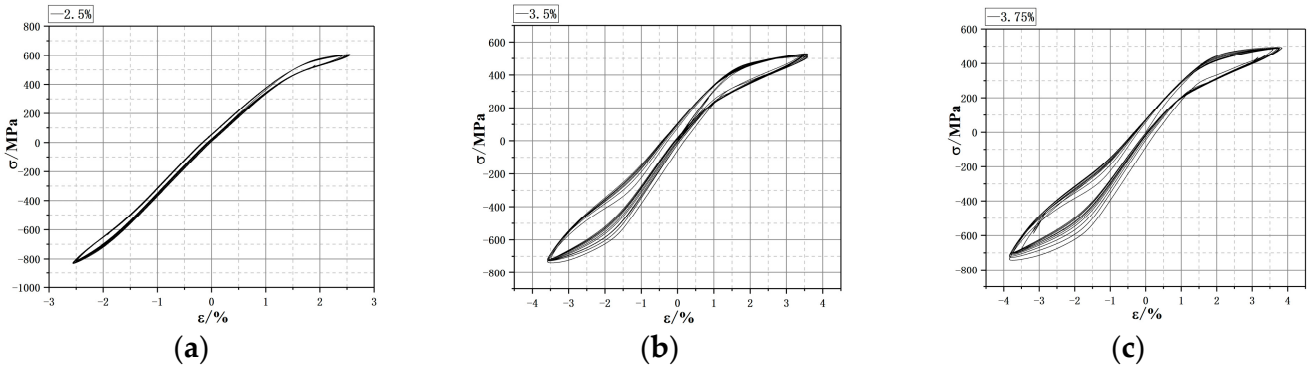


**Figure 6.** Effect of strain amplitude on stress–strain relationship: (**a**) Strain amplitude of ±2.5%; (**b**) strain amplitude of ±3.5%; (**c**) strain amplitude of ±3.75%.

To investigate the changes in the residual strain and energy dissipation level of SMA bars with the increase in cycle times at different strain amplitudes, the residual strain and energy dissipation capacity of specimens under different strain amplitudes were analyzed by taking cycle times as abscissa (as shown in Figure 7). Figure 7 shows that when the strain amplitude is 2.5%, the energy dissipation and residual strain are very small and almost keeps constant with the increase in cycle times. When the strain amplitude is 3.5%, the residual strain of the specimen increases from 0.29% to 0.43%, with an increase of 48.3%; the energy consumption of the specimen decreases from 107.42 KN·mm to 93.16 KN·mm, with a decrease of 13.3%. When the strain amplitude is 3.75%, the residual strain of the specimen increases from 0.22% to 0.33%, with an increase of 50%; the energy consumption of the specimen decreases from 124.27 KN·mm to 99.65 KN·mm, with a decrease of 19.8%.

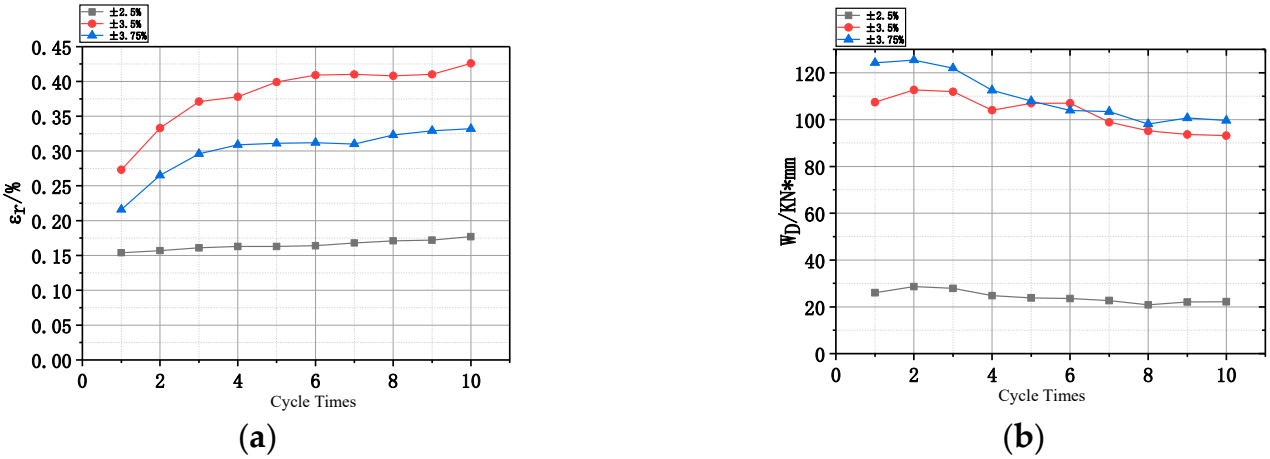


**Figure 7.** Effect of strain amplitude on residual strain and energy dissipation: (**a**) Effect of strain amplitude on residual strain; (**b**) effect of strain amplitude on energy consumption.

The residual strain of SMA bars at the strain amplitude of ±3.5% lies between it at a strain amplitude of ±2.5% and ±3.75%; then, the test results are in accordance with the basic law. However, the test results deviate near the sixth cycle when the strain amplitude is ±3.5%. The reasons for this are as follows: firstly, the specimens used in this test are slightly different in size from the low-circumference fatigue standard specimen, so there is a size effect. The second is that the processing quality of SMA material is slightly unstable, and the internal lattice microstructure of the material itself has an influence.

The test results show that the SMA bar with a diameter of 14 mm has small residual strain, good recovery performance and certain energy dissipation capacity under a low-cyclic reciprocating load.

### *4.2. Influence of Cyclic Loading Times on the Superelastic and Energy Dissipation Properties of SMA Bars*

The SMA bar (specimen 3) which underwent a heat treatment condition of being held at 350 °C for 30 min was cycled for 5, 10, 20 and 30 turns with a ±3.75% strain amplitude, and its stress–strain hysteresis curves were plotted (Figure 8a–d).

It can be seen from Figure 8 that (1) when the strain amplitude is ±3.75%, the negative stress of the specimen has an obvious degradation process during cyclic loading, but the degradation of the positive stress is not obvious. (2) The area of the hysteresis curve gradually decreases with the increase in cycle times, which means that the energy consumption of the specimen gradually decreases with the increase in cycle loading times.

Figure 9 shows the variation trend of residual stress and the single-cycle energy consumption of specimen 3 with the increase in cycle times during loading: with the increase in cyclic loading times, the residual strain of the specimen gradually rises until it is stable, and the maximum residual strain in the cyclic process is about 0.4%. The energy consumption of a single cycle gradually decreases until it is stable, and the energy consumption of a single cycle is at least 75 KN·mm. According to the test results, the SMA bar with the diameter of 14 mm has a certain energy dissipation capacity and recovery performance under a reciprocating load.

Figure 10 shows the trend of the peak stress of specimen 3 with the increase in cycling period in the process of cyclic loading: when the strain amplitude is 3.75%, the maximum tensile stress of specimen remains stable, and the maximum compressive stress has a decreasing trend in the early stage of loading and gradually stabilizes after a certain cycle. It can be seen that during the loading process, the specimen first presents a certain degree of cyclic softening and then enters the cyclic stable state.

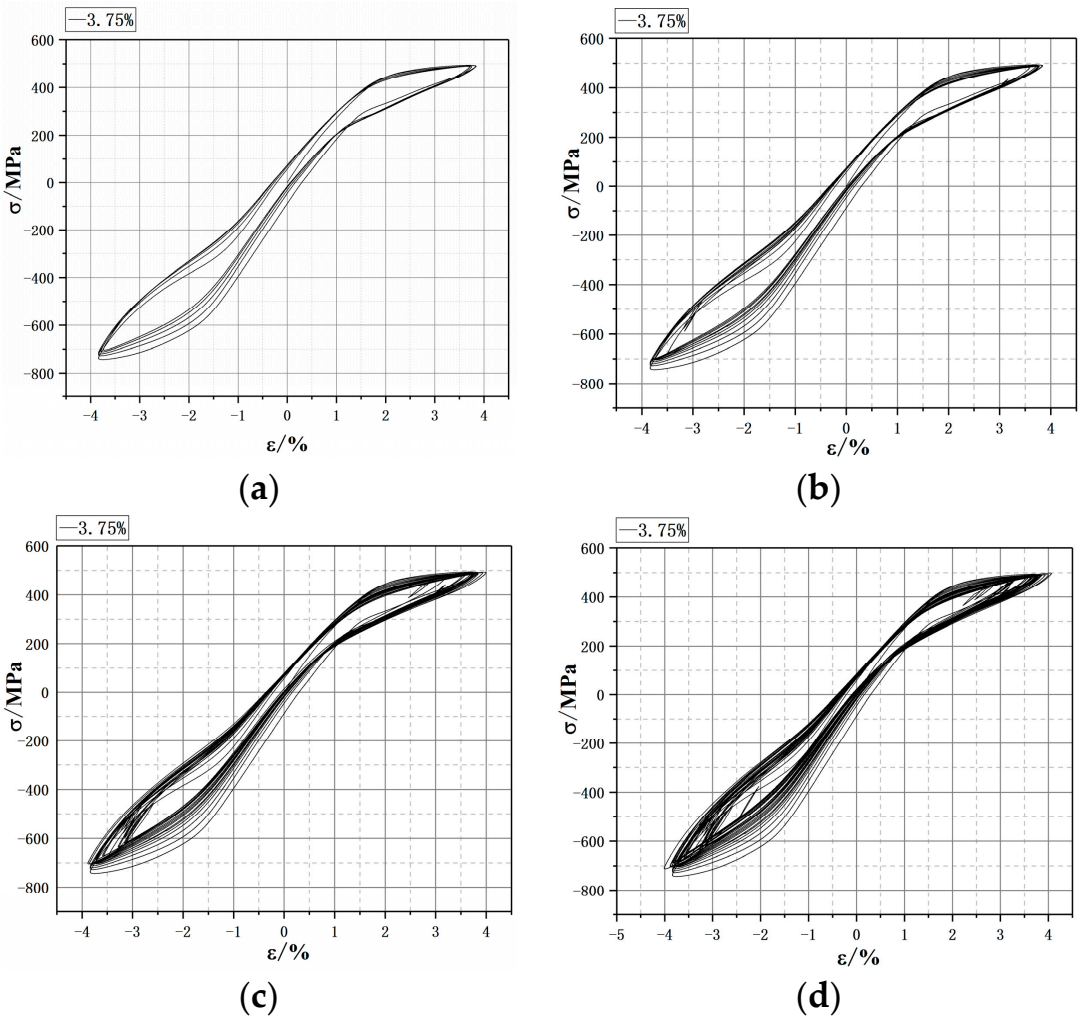


**Figure 8.** Influence of cyclic loading times on the stress–strain relationship: (**a**) 5-week cycle at ±3.75% of amplitude; (**b**) 10-week cycle at ±3.75% of amplitude; (**c**) 20-week cycle at ±3.75% of amplitude; (**d**) 30-week cycle at ±3.75% of amplitude.

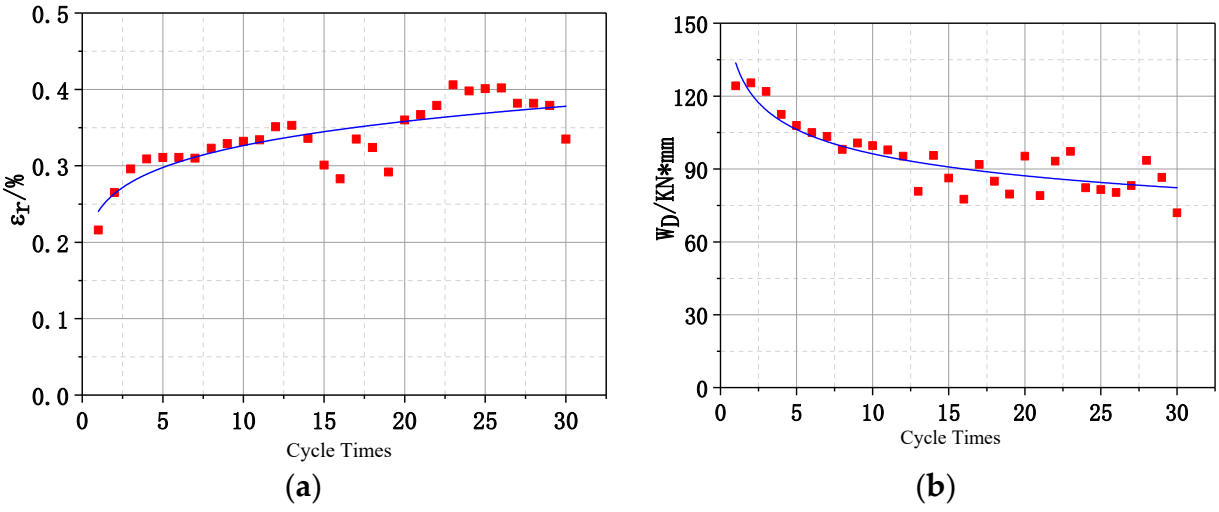


**Figure 9.** Trend of residual strain and energy dissipation of the specimen with increasing number of cycles; (**a**) effect of cycle number on residual strain; (**b**) effect of cycle number on energy consumption.

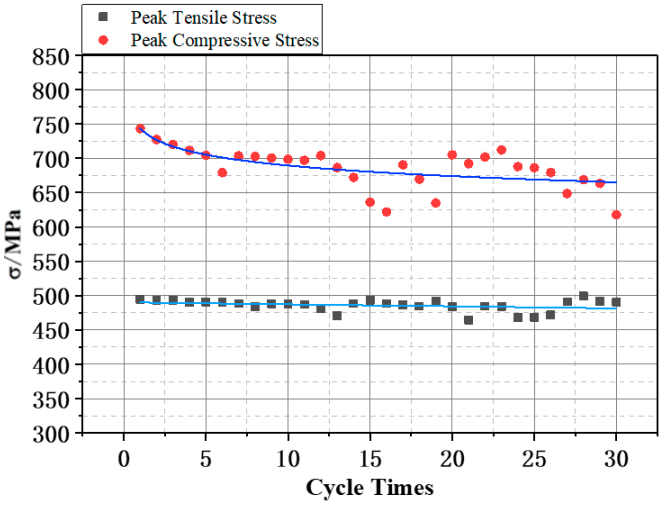


**Figure 10.** Comparison of peak stress variation at different numbers of cycles.

### *4.3. Influence of Heat Treatment Parameters on Superelasticity and Energy Consumption of SMA Bar*

The SMA bars, after three different heat treatments of being held at 350 °C for 30 min, held at 400 °C for 15 min and held at 400 °C for 30 min, were subjected to a low-circumferential fatigue test with a strain amplitude of ±2.5%, and their stress–strain hysteresis curves are shown in Figure 11. From the test data, the residual strains of the three specimens with different heat treatments are 0.15%, 0.12% and 0.05%; the energy dissipation values are 26.03 kN·mm, 47.15 kN·mm and 41.77 kN·mm. In summary, the SMA bars with the heat treatment of being held at 400 °C for 15 min have the best performance.

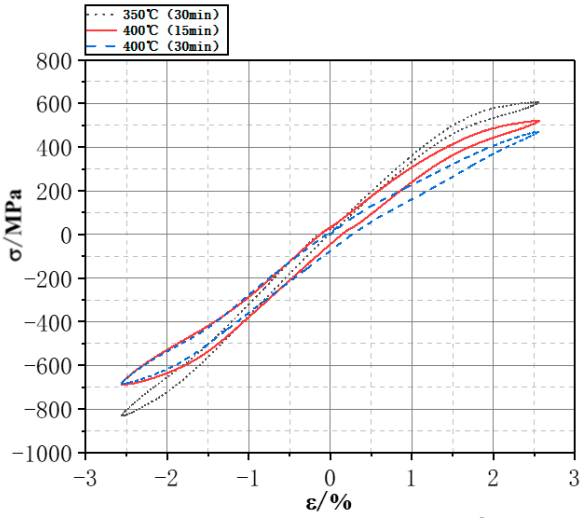


**Figure 11.** Effect of heat treatment parameters on stress–strain relationship.

## 5. FEA

According to the experimental data, the Auricchio multi-linear simplified model in ABAQUS [22,23] was used to simulate the low-cycle fatigue performance of SMA bar with the heat treatment parameters of being held at 350 °C for 30 min, and the comparison of the stress–strain curve and nephogram between the finite element and experiments are shown in Figures 12 and 13.

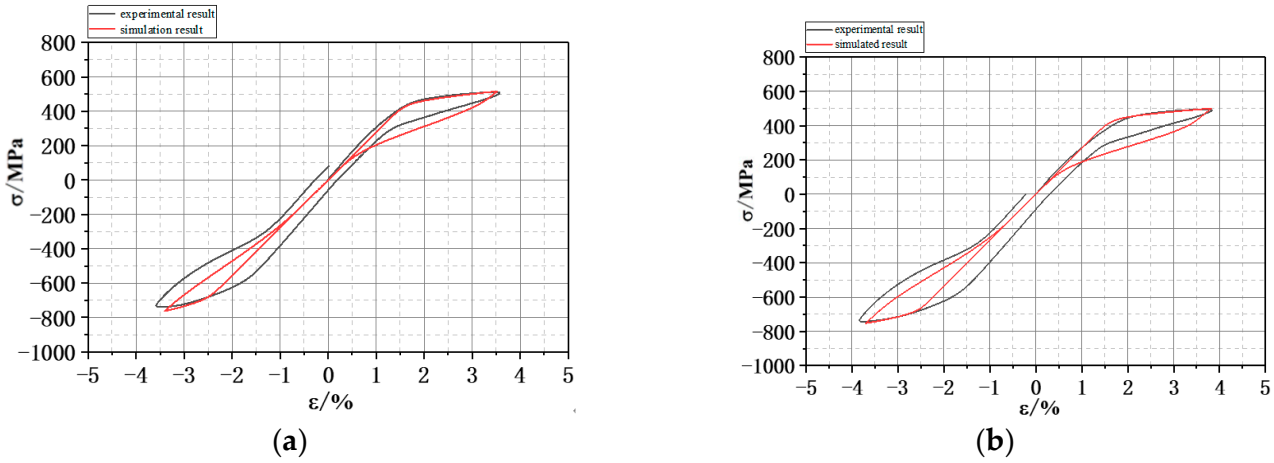


**Figure 12.** Comparison of experimental results and simulation results of stress–strain curve: (**a**) Strain amplitude of ±3.5%; (**b**) strain amplitude of ±3.75%.

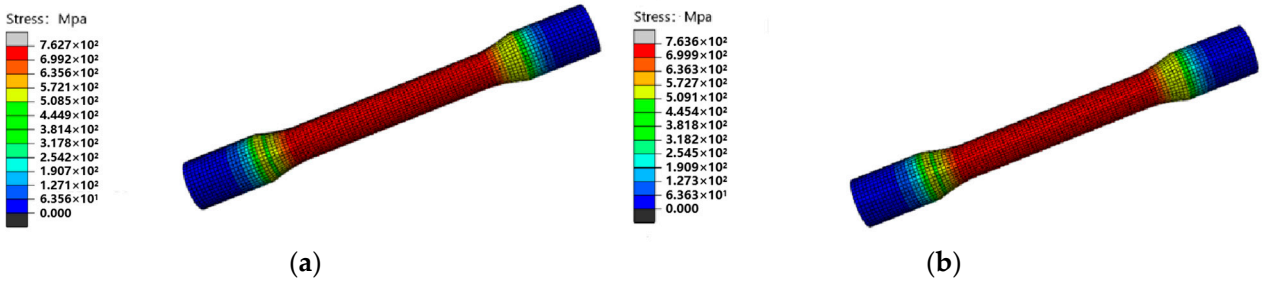


**Figure 13.** SMA bar axial strain nephogram: (**a**) Stress amplitude of ±3.5%; (**b**) stress amplitude of ±3.75%.

The comparative analysis of the mechanical parameters in Table 4 shows that the error of the stress peak between the experimental results and the simulated analysis is within 5%, which means that the finite element simulation results are in better agreement with the experimental results. However, the energy consumption error is relatively large because the fatigue caused by the small deformation observed in the test is not considered in the numerical simulations. Moreover, a larger hysteresis loop area and increased energy consumption result from the residual strain in the specimen. Generally, the stress–strain hysteresis curves obtained from the finite element simulation are in good agreement with the stress–strain curves obtained from the tests, so it is feasible to use ABAQUS2021 to simulate the low-circumference fatigue of the shape-memory alloy bars.

**Table 4.** Comparative analysis of mechanical parameters.

| Specimen Type | Type of Parameter | Single-Week Energy Consumption (kN·mm) | Tensile Stress Peak (MPa) | Compressive Stress Peak (MPa) |
|---|---|---|---|---|
| Strain Amplitude of ±3.5% | Experiment | 107.42 | 507.1 | 738.1 |
| | Simulation | 56.29 | 505.2 | 752.7 |
| | Error | 47% | 0.37% | 1.98% |
| Strain Amplitude of ±3.75% | Experiment | 124.27 | 491.1 | 743.2 |
| | Simulation | 76.3 | 500.7 | 752.4 |
| | Error | 38.60% | 1.95% | 1.23% |

## 6. Conclusions

In this paper, the influences of strain amplitude, cycle times and heat treatment conditions on the fatigue properties of shape-memory alloy bars with the diameters of

14 mm were studied by using a low-cycle fatigue test method. The results show the energy dissipation capacity and small residual strain of the SMA bars under low cyclic fatigue loading, implying that SMA bars can be used as self-centering energy-dissipating elements in seismic design. The following conclusions are obtained:

(1). With the increase of strain amplitude, the energy dissipation performance of SMA bars shows an overall upward trend, and the residual strain is relatively small at the strain amplitude of 3.5% and 3.75%.
(2). In the test, with the increase of loading times, the peak compressive stress of SMA bars gradually tends to be stable after obvious degradation, the energy consumption of a single cycle decreases and the residual strain increases.
(3). The heat treatment parameters affect the energy dissipation and residual strain of shape-memory alloys. Larger energy dissipation and smaller residual strain of the SMA bar are obtained at 400 °C for 15 min.

**Author Contributions:** L.L.: Supervision, Conceptualization; Investigation, Formal analysis, Writing-original draft. X.Z.: Conceptualization, Formal analysis, Writing—Review & Editing. J.C.: Supervision, Writing—Review & Editing. All authors have read and agreed to the published version of the manuscript.

**Funding:** Science Foundation in the Henan province (Grant No.192102210030 and 182102210439) and the National Science Foundation in China (NSFC) (Grant No.U1404524). Tackle-Key-Program of S&T Committee of Henan Province in China (Grant No. 202102210209). Key-Research-Projects of Higher Education Institutions of Henan Province in China (Grant No. 23A590002). Key R&D Special Projects of Henan Province in China (Grant No. 221111230700).

**Data Availability Statement:** This paper is new. Neither the data nor any part of its content have been published or have been accepted elsewhere.

**Conflicts of Interest:** The authors declare no conflict of interest.

## References

1. Graesser, E.J.; Cozzarelli, F.A. Shape-Memory Alloys as New Materials for Aseismic Isolation. *J. Eng. Mech.* **1991**, *117*, 2590–2608. [CrossRef]
2. Piedboeuf, M.C.; Gauvin, R.; Thomas, M. Damping behaviour of shape memory alloys: Strain amplitude, frequency and temperature effects. *J. Sound. Vib.* **1998**, *214*, 885–901. [CrossRef]
3. Dolce, M.; Cardone, D. Mechanical behaviour of shape memory alloys for seismic applications 2. Austenite NiTi wires subjected to tension. *Int. J. Mech. Sci.* **2001**, *43*, 2657–2677. [CrossRef]
4. Gong, J.; Tobushi, H. Superelastic deformation behavior of TiNi shape memory alloy subjected to various cyclic loading. *J. Funct. Mater.* **2002**, *33*, 391–393+397.
5. Gong, J.; Tobushi, H.K.; Takada, K.; Okumura, K. Analysis and simulation on cyclic superelastical deformation behavior of TiNi shape memory alloy subjected to loading and unloading. *J. Aeronaut. Mater.* **2002**, *22*, 6–12.
6. Sadiq, H.; Wong, M.B.; Al-Mahaidi, R.; Zhao, X.L. The effects of heat treatment on the recovery stresses of shape memory alloys. *SMArt Mater. Struct.* **2010**, *19*, 035021. [CrossRef]
7. Tamai, H.; Kitagawa, Y. Pseudoelastic behavior of shape memory alloy wire and its application to seismic resistance member for building. *Comp. Mater. Sci.* **2002**, *25*, 218–227. [CrossRef]
8. Zuo, X.; Li, A.; Ni, L.; Chen, Q. An Experimental Study On The Mechanical Behavior Of Superelastic Niti Shape Memory alloy Wires. *J. China Civ. Eng.* **2004**, *37*, 10–16.
9. Qian, H.; Li, J.; Li, H.; Chen, H. Mechanical behavior tests of NiTi wires with different diameters for structural vibration control. *J. Vib. Shock.* **2013**, *32*, 89–95.
10. Li, G.; Cui, D.; Hong, S. Experimental Investigation on Mechanical Properties of New Form Super-elastic Shape Memory AlloyWires. *J. Dalian Univ.* **2008**, *29*, 129–133.
11. Yan, S.; Wang, Q.; Wang, W. Experimental Research on Mechanical Performance for Pseudo-Elasticity of Shape Memory Alloy. *J. Shenyang Jianzhu Univ. (Nat. Sci.)* **2010**, *26*, 458–463.
12. Chen, W.W.; Wu, Q.P.; Kang, J.H.; Winfree, N.A. Compressive superelastic behavior of a NiTi shape memory alloy at strain rates of 0.001-750 s-1. *Int. J. Solids Struct.* **2001**, *38*, 8989–8998. [CrossRef]
13. Dolce, M.; Cardone, D. Mechanical behaviour of shape memory alloys for seismic applications 1. Martensite and austenite NiTi bars subjected to torsion. *Int. J. Mech. Sci.* **2001**, *43*, 2631–2656. [CrossRef]
14. Desroches, R.; Mccormick, J.; Liu, S.C. Properties of large-diameter shape memory alloys under cyclical loading. *Proc. Spie.* **2003**, *5057*, 187–196.

15. Wang, W.; Fang, C.; Liu, J. Large size superelastic SMA bars: Heat treatment strategy, mechanical property and seismic application. *Smart Mater. Struct.* **2016**, *25*, 075001. [CrossRef]
16. Zheng, B.-Y.; Shang, Z.-J.; Wang, Z.-M. Effects of Loading Rates on the Mechanical Behavior of Superelastic TiNi Shape Memory Alloy Bars. *Mech. Sci. Technol. Aerosp. Eng.* **2008**, *27*, 1236–1238+1242.
17. Ren, W.; Wang, L.; Jia, J.; Jia, R. Experimental study on mechanical behavior of superelastic shape memory alloy bar. *J. Funct. Mater.* **2013**, *44*, 258–261.
18. Dong, J. Experimental Research on the Self-centering Device Based on Large Diameter SMA. *Struct. Eng.* **2018**, *34*, 101–108.
19. Kang, L.; Qian, H.; Guo, Y.; Li, Z. Experimental investigation on mechanical properties of large size shape memory alloy bars underdifferent heat treatments. *J. Funct. Mater.* **2021**, *52*, 1185–1191.
20. Wang, W.; Shao, H. Experimental Investigation on Mechanical Properties of Shape Memory Alloy Bars in Different Sizes. *Struct. Eng.* **2014**, *30*, 168–174.
21. Zhuang, P.; Xue, S.; Wei, J.; Liu, Y. Research on Mechanical Performance of Superelastic NiTi Shape Memory Alloy Bars. *J. Archit. Civ. Eng.* **2015**, *32*, 96–103.
22. Tian, L.M.; Li, M.H.; Li, L.; Li, D.Y.; Bai, C. Novel joint for improving the collapse resistance of steel frame structures in column-loss scenarios. *Thin-Walled Struct.* **2023**, *182*, 110219. [CrossRef]
23. Tian, L.M.; Wei, J.P.; Huang, Q.X.; Woody, J. Collapse-Resistant Performance of Long-Span Single-Layer Spatial Grid Structures Subjected to Equivalent Sudden Joint Loads. *J. Struct. Eng.* **2021**, *147*, 04020309. [CrossRef]